

# In situ separation of root hydraulic redistribution of soil water from liquid and vapor transport

Jeffrey M. Warren · J. Renée Brooks ·  
Maria I. Dragila · Frederick C. Meinzer

Received: 7 April 2010 / Accepted: 18 February 2011 / Published online: 13 March 2011  
© Springer-Verlag (outside the USA) 2011

**Abstract** Nocturnal increases in water potential ( $\psi$ ) and water content ( $\theta$ ) in the upper soil profile are often attributed to root water efflux, a process termed hydraulic redistribution (HR). However, unsaturated liquid or vapor flux of water between soil layers independent of roots also contributes to the daily recovery in  $\theta$  ( $\Delta\theta$ ), confounding efforts to determine the actual magnitude of HR. We estimated liquid ( $J_l$ ) and vapor ( $J_v$ ) soil water fluxes and their impacts on quantifying HR in a seasonally dry

ponderosa pine (*Pinus ponderosa*) forest by applying existing datasets of  $\psi$ ,  $\theta$  and temperature ( $T$ ) to soil water transport equations. As soil drying progressed, unsaturated hydraulic conductivity declined rapidly such that  $J_l$  was irrelevant ( $<2E-05$  mm h<sup>-1</sup> at 0–60 cm depths) to total water flux by early August. Vapor flux was estimated to be the highest in upper soil (0–15 cm), driven by large  $T$  fluctuations, and confounded the role of HR, if any, in nocturnal  $\theta$  dynamics. Within the 15–35 cm layer,  $J_v$  contributed up to 40% of hourly increases in nocturnal soil moisture. While both HR and net soil water flux between adjacent layers contribute to  $\theta$  in the 15–65 cm soil layer, HR was the dominant process and accounted for at least 80% of the daily recovery in  $\theta$ . The absolute magnitude of HR is not easily quantified, yet total diurnal fluctuations in upper soil water content can be quantified and modeled, and remain highly applicable for establishing the magnitude and temporal dynamics of total ecosystem water flux.

This manuscript has been authored by UT-Battelle, LLC, under Contract No. DE-AC05-00OR22725 with the U.S. Department of Energy. The United States Government retains and the publisher, by accepting the article for publication, acknowledges that the United States Government retains a non-exclusive, paid-up, irrevocable, world-wide license to publish or reproduce the published form of this manuscript, or allow others to do so, for United States Government purposes.

**Electronic supplementary material** The online version of this article (doi:10.1007/s00442-011-1953-9) contains supplementary material, which is available to authorized users.

J. M. Warren (✉)  
Environmental Sciences Division,  
Oak Ridge National Laboratory,  
Oak Ridge, TN 37831-6301, USA  
e-mail: warrenjm@ornl.gov

J. M. Warren · F. C. Meinzer  
PNW Research Station, USDA Forest Service,  
Corvallis, OR 97331, USA

J. R. Brooks  
Western Ecology Division, US EPA/NHEERL,  
200 SW 35th St, Corvallis, OR 97333, USA

M. I. Dragila  
Department of Crop and Soil Science,  
Oregon State University, Corvallis, OR 97331, USA

**Keywords** Diffusivity · Hydraulic lift · Ponderosa pine · Hydraulic conductivity · Vapor flow

## Introduction

Hydraulic redistribution (HR) is a passive process in which roots take up water from moist soil, transport it through the soil profile following a water potential gradient, and then release it into drier soil (Richards and Caldwell 1987). This process often occurs at night when plant canopy transpiration is minimized, which reduces aboveground plant demand for water and allows drier soil layers to compete as a sink for root water. The process of HR is a widespread phenomenon that has been reported in herb, grass, shrub and tree root and mycorrhizal hyphal systems in both mesic

and xeric environments (Caldwell et al. 1998; Querejeta et al. 2003; Espeleta et al. 2004; Meinzer et al. 2004; Warren et al. 2008). HR has been identified and quantified by transport and accumulation patterns of stable or enriched isotopes (Caldwell and Richards 1989; Dawson 1993; Brooks et al. 2006), reversal of root sap flow away from the stem (Burgess et al. 2000) and by diurnal fluctuations in soil water potential ( $\psi$ ) and water content ( $\theta$ ) (Fig. 1) (Brooks et al. 2002; Warren et al. 2007). However, absolute quantification of HR has been difficult, since diurnal changes in  $\theta$  are at least partially due to concurrent soil liquid or vapor water flux independent of roots. In addition, accurate measurement of the minute fluctuations in  $\theta$  that represent both HR and soil water transport is difficult, and instrument sensitivity can be affected by the environmental gradients that drive water transport (especially temperature;  $T$ ) that can lead to over-, or under-estimation of actual values. The absolute magnitude of HR is thus elusive, yet by modeling soil water transport independent of roots and comparing results with in situ measured water fluxes, the relative contribution of HR to diurnal changes in  $\theta$  can be further refined.

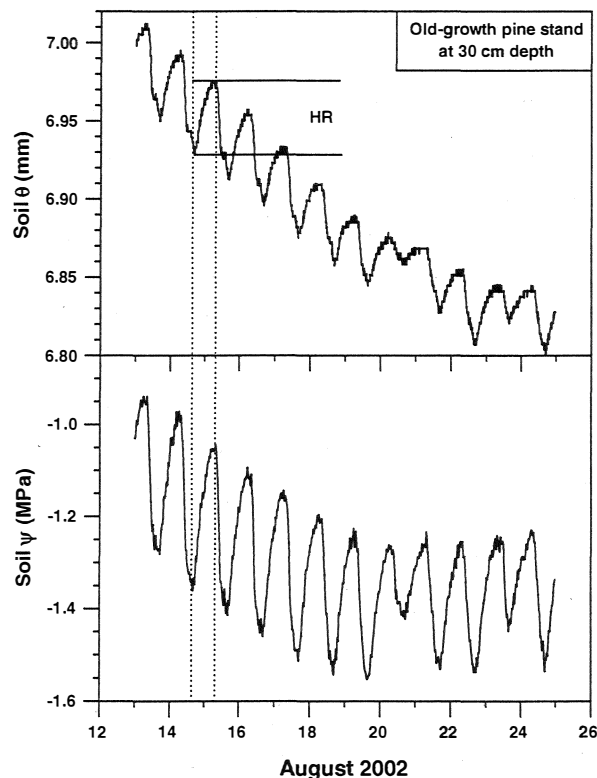


**Fig. 1** Diurnal patterns of measured soil water content ( $\theta$ ) and soil water potential ( $\psi$ ) at a depth of 30 cm across several weeks in August for an old-growth *Pinus ponderosa* stand. Daily recovery of  $\theta$  has been used as an indicator of root hydraulic redistribution of soil water (HR). Note the synchronized response of  $\theta$  and  $\psi$  to cloudy conditions on days 20 and 23

Based on daily recovery in  $\theta$  ( $\Delta\theta$ ), mean maximum reported rates of HR for an old-growth *Pinus ponderosa* stand were  $3.0 \text{ E-}04 \text{ cm}^3 \text{ cm}^{-3} \text{ day}^{-1}$  ( $0.15 \text{ mm day}^{-1}$ ) in the upper 15–65 cm profile, with rates up to  $1.2 \text{ E-}03 \text{ cm}^3 \text{ cm}^{-3} \text{ day}^{-1}$  at specific locations (Warren et al. 2007). As the summer drying cycle proceeded, transport of water from deep sources into the upper profile via roots began when  $\psi$  in the upper soil declined to  $-0.05$  to  $-0.30 \text{ MPa}$ , depending on soil characteristics. Once evapotranspiration depleted the soil moisture to this critical water potential threshold, HR was generally observed until seasonal autumn rains minimized soil  $\psi$  gradients. At night, or under conditions of low transpirational demand (e.g., cloudy, low vapor pressure deficit),  $\psi$  gradients between the trees and upper soil layer can be smaller than  $\psi$  gradients within the soil, and water is moved via roots from wetter soil layers to drier soil layers, which results in parallel increases in soil  $\psi$  and  $\theta$  (Fig. 1). However, the magnitude of those increases also reflects net inputs of liquid or vapor soil water movement independent of roots as affected by vertical variability in soil physical properties,  $T$ ,  $\psi$  and moisture patterns.

Liquid transport of soil water in the absence of roots is primarily driven by  $\psi$  gradients and influenced by soil physical properties, especially bulk density ( $\rho_b$ ) and particle size distribution (Campbell 1985; Selker et al. 1999). Unsaturated soil hydraulic conductivity ( $k$ ) controls the flow of liquid water from deep moist soil layers to drier upper layers following a  $\psi$  gradient, and since  $k$  is a function of  $\theta$ ,  $k$  drops exponentially as soils dry. When soils are moist and  $k$  is high, soil water removed from the upper profile by evapotranspiration can increase relative  $\psi$  gradients within the profile and drive liquid water flux between layers. However, during a drying period, exponential declines in soil diffusivity ( $D$ ) and  $k$  increasingly limit liquid water transport. At this point, vapor flux becomes a much larger component of the net water transport between layers (Philip 1957; Campbell 1974). Vapor transport of water within the soil is primarily driven by  $T$  gradients, with flow moving from warmer to cooler areas of the soil (Philip and de Vries 1957). At night, cooling of the soil surface can lead to condensation of moisture in the upper layers if the dew point  $T$  is reached. Water vapor may even be directly absorbed by soil particles in the absence of condensation (Agam (Ninari) and Berliner 2004).

The daily recovery in upper soil  $\theta$  can be lost the following day, as temperature-driven increases in vapor pressure deficit result in significant evaporative loss. This diurnal cycling of water flux into and out of the upper soil can have the same appearance as HR, and thus quantification of HR can be difficult where gradients in  $\psi$  and  $T$  exist. Indeed, during the summer, the upper soil is often

subjected to large diurnal  $T$  fluctuations that regulate water transport between the upper soil and the atmosphere, and between the upper and lower soil layers. Net vapor transport at a specific depth can oscillate between upward and downward flux depending upon relative magnitudes of the  $T$  gradients, and can be opposite to the direction of concurrent unsaturated liquid water transport (Philip and de Vries 1957; Nakayama et al. 1973).

Diurnal increases in  $\theta$  similar to HR have been reported in bare agricultural soil devoid of plants, which substantiates the process of water flux independent of roots, albeit only the uppermost soil layers have been studied (0–15, 0–9 or 0–7 cm, respectively; Rose 1968a; Jackson 1973; Bittelli et al. 2008). In those studies, soil  $\theta$  in the top 0–1.5 cm layer increased  $0.01\text{--}0.10\text{ cm}^3\text{ cm}^{-3}\text{ day}^{-1}$ , driven by diurnal  $T$  fluctuations ranging from 20 to 40°C. The increase in  $\theta$  was attributed to  $T$ -dependent downward vapor flux in spite of greater  $\theta$  at depth.

This study models the components of soil water flux within upper soil layers (15–65 cm) in a mature pine forest to separate root and soil contributions to diurnal patterns of  $\theta$ . The objectives were to evaluate vapor ( $J_v$ ) and liquid ( $J_l$ ) water flux density between upper soil layers during periods of measured nocturnal increases in  $\theta$  to investigate how much of the diurnal increase in soil moisture may be attributable to soil versus root processes. Concurrent measurements of  $\psi$ ,  $\theta$ , and  $T$  in adjacent soil layers (10–20, 20–30, 30–40, 40–50, 50–60, 60–70 cm) collected across a growing season, and knowledge of soil physical characteristics ( $\rho_b$ , texture, soil water retention curves) in each layer provided the input parameters for the modeling exercise.

## Materials and methods

### Site description

The stand was located within the Metolius Research Natural Area within the Deschutes National Forest in central Oregon, USA (44°30'N, 121°37'W) at an elevation of 915 m. The stand was predominantly comprised of dominant, old-growth ponderosa pine (*P. ponderosa* Dougl. ex Laws.) trees, mixed-age regenerating trees <100 years old, and a sparse understory that allowed solar penetration to the forest floor. Soil at the site is an Alfic Vitrixerand, consisting of a loamy sand at 20 cm (77% sand, 19% silt, 4% clay) that transitioned to a sandy loam at 60 cm (71% sand, 23% silt, 6% clay) (Law et al. 1999, 2001). The forest floor was comprised of a thin layer of pine needle litter underlain by a crumbly organic soil layer (0–5 cm deep); mineral soils beneath this layer were low in organic matter (Law et al. 2001). The water table and rooting depth were

below 2.5 m at the site during the study period, based on prior observations. The site is seasonally dry with less than 50 mm of precipitation during the growing season that results in significant upper soil drying. Detailed descriptions of the study site, soil properties, spatial heterogeneity of  $\psi$  and  $\theta$ , and methodologies employed have been previously reported (Warren et al. 2005, 2007). Data have been collected from this site since 2000; however, data used for this analysis were derived from the relatively complete 2002 dataset, which included a dry summer with only 18 mm of rain through the growing season.

### Soil temperature and water potential

Soil water potential ( $\psi$ ) and  $T$  were measured using four replicate thermocouple-psychrometer arrays (PST-55; Wescor, Logan, UT, USA), individually calibrated, and installed into the soil at depths of 20, 30, 40, 50, 60 and 100 cm (Warren et al. 2005). Soil  $T$  and  $\psi$  were measured every 30 min, with a 30-s cooling time to accommodate the Peltier effect, and data were recorded by a solar-insulated data logger (CR-7; Campbell Scientific, Logan, UT, USA). Soil  $\psi$  at 2 and 10 cm was modeled by nonlinear regression ( $\psi = y_0 + a(1 - \exp^{-bx})$ ) fit to measured  $\psi$  from  $x = 20\text{--}100$  cm depth at DOY 210, 240 and 270. The 90% CI surrounding mean  $\psi$  was used to generate the range of possible values of  $\psi$  at 2 and 10 relative to measured  $\psi$  at 20 cm. Soil  $T$  data from 2, 8 and 15 cm depths (six replicates) were obtained from a concurrent, ongoing study of carbon and water flux at the site (Irvine et al. 2002) and were interpolated to estimate soil  $T$  at 2 and 10 cm for use in water flux calculations (below).

### Soil volumetric water content

Soil volumetric water content,  $\theta$ , was quantified using multi-sensor, frequency domain capacitance (FDC) probes (EnviroSCAN; Sentek., Adelaide, Australia) that were carefully installed following the manufacturer's guidelines (Brooks et al. 2002; Warren et al. 2005). The sensors operate at high frequency (100–150 MHz depending on  $\theta$ ), which may reduce errors associated with salinity and acidity (Paltineanu and Starr 1997), and above the 30 MHz minimum below which the frequency directly impacts apparent permittivity (Dean et al. 1987). Four replicate probes were installed in sealed PVC access tubes, with sensors spaced at 20, 30, 40, 50, 60 and 100 cm depths. Each capacitance sensor was frequency-normalized by calibration against air and water in the laboratory to ensure the precision of measurements, and field calibration enhanced the accuracy of measurements (Morgan et al. 1999; Warren et al. 2005). Volumetric water content was measured every 10 min and recorded by a data logger

(model RT6; Sentek).  $\theta$  values were averaged every 30 min for vapor and liquid water flux calculations. Soil  $\theta$  at 2 and 10 cm was modeled based on linear ( $\theta = a + bx$ ) or, in some cases, quadratic regressions fit to measured  $\theta$  from  $x = 20$ – $40$  cm depth for each probe for DOY 210, 240 and 270.

Large shifts in soil  $T$  can impact both soil permittivity and response of capacitance sensors, thereby confounding the small fluctuations in  $\theta$  attributable to HR. Thus,  $\theta$  was adjusted when soil  $T$  differed from the laboratory calibration  $T$  ( $20^\circ\text{C}$ ). The  $T$  adjustment was based on previous comprehensive calibrations across soil  $\theta$  for a portable capacitance sensor operating at 60 MHz (Kuráň 1982). We validated the use of these calibrations by additional testing of multiple 150 MHz sensors in moistened sand exposed to a  $5$ – $20^\circ\text{C}$   $T$  gradient (ESM1, Online Resource). The Kuráň calibrations used site-specific residual ( $\theta_r$ ; for very dry soil) and saturated ( $\theta_s$ ) soil water contents (Table 1). The  $T$  correction factor for  $\theta$  ( $\Delta\theta_T$ ;  $\text{cm}^3 \text{cm}^{-3} \text{ }^\circ\text{C}^{-1}$ ) was individually calculated for each depth range based on a linear regression between  $\Delta\theta_T$  and  $\theta/\theta_s$ , and assumed  $\Delta\theta_T$  (at  $\theta_r$ ) = 0,  $\Delta\theta_T$  (at  $0.5\theta_s$ ) = 0.0014, and  $\Delta\theta_T$  (at  $\theta_s$ ) = 0.003 (Kuráň 1982):

$$10 - 20 \text{ cm} : \Delta\theta_T = -0.0001653 + 0.003159(\theta/\theta_s) \quad (1.1)$$

$$30 \text{ cm} : \Delta\theta_T = -0.0002294 + 0.003235(\theta/\theta_s) \quad (1.2)$$

$$40 \text{ cm} : \Delta\theta_T = -0.0002385 + 0.003246(\theta/\theta_s) \quad (1.3)$$

$$50 \text{ cm} : \Delta\theta_T = -0.0002433 + 0.003251(\theta/\theta_s) \quad (1.4)$$

$$60 \text{ cm} : \Delta\theta_T = -0.0007794 + 0.003863(\theta/\theta_s) \quad (1.5)$$

The correction factors were then applied to measured soil moisture content at each depth:

$$\theta_{corrected} = \theta + \theta \times \Delta\theta_T \times (20^\circ\text{C} - T). \quad (2)$$

#### Calculation of vapor and liquid water flux

Vapor flux ( $J_v$ ) within the upper soil layers was determined during periods of HR to investigate how much of the diurnal increase in soil moisture may have been attributable to water vapor flux. Model input included concurrent measurements of  $\psi$ ,  $\theta$ , and  $T$  from adjacent soil layers (10–20, 20–30, 30–40, 40–50, 50–60, 60–70 cm) and bulk densities of each layer.  $J_v$  was also modeled between the 10 and 2 cm soil layers using measured  $T$ , regression estimates of  $\psi$  and  $\theta$ , and assuming soil water retention characteristics equal to those measured at 20 cm. It was not our goal to characterize the dynamics of vapor flux in the soil apart from its contribution to apparent HR.

Soil water vapor transport is driven by vapor pressure differences and thermal gradients, with vapor movement from warmer to cooler areas of the soil (Philip and de Vries 1957)

$$J_v = -D \frac{\Delta\rho_v}{\Delta x} - Dh_r s \eta \frac{\Delta T}{\Delta x}. \quad (3)$$

The first term of Eq. 3 expresses Fick's first law for isothermal vapor flux between two points in the soil, where  $D$  is the diffusion coefficient in soil,  $\Delta\rho_v$  is the water vapor density difference, and  $\Delta x$  is the distance between measurement points.  $D$  is affected by air permeability in the soil, which in turn is affected by water content and soil structural characteristics such as pore size. Early diffusion coefficient models (e.g., Penman 1940) have been substantially improved to include more parameters and dependency on the soil water retention curves, which we

**Table 1** Soil physical and hydraulic characteristics in the old-growth ponderosa pine stand

Depth (cm)	Bulk density $\rho_b$ ( $\text{g cm}^{-3}$ )	Range $\Delta T^a$ ( $^\circ\text{C}$ )	Maximum $\Delta\psi^a$ (MPa)	Residual $\theta^b$ $\theta_r$ ( $\text{cm}^3 \text{cm}^{-3}$ )	Saturated $\theta^b$ $\theta_s$ ( $\text{cm}^3 \text{cm}^{-3}$ )	Soil water retention parameter ( $b$ )	Characteristic soil texture parameter <sup>d</sup> ( $\lambda$ )	Saturated conductivity <sup>e</sup> $k_s$ (cm/h)
10	1.04	−17.3 to 8.6	3.30	0.025	0.50	6.5	0.282	34.6
20	1.04	−7.3 to 6.5	0.95	0.025	0.50	6.5	0.282	34.6
30	1.09	−2.8 to 1.3	0.50	0.035	0.48	5.7	0.305	18.9
40	1.14	−1.8 to 0.4	0.37	0.035	0.46	5.1	0.287	11.3
50	1.19	−1.5 to 0.1	0.73	0.035	0.45	5.8	0.214	7.98
60	1.24	−1.5 to 0.0	0.43	0.105	0.43	9.3	0.308	6.00

<sup>a</sup> Seasonal differences reached with adjacent upper layer; e.g., 10 cm depth = (values at 10 cm) − (values at 2 cm); 20 cm depth = 20–10, etc. Negative values indicate  $T$  is lower at depth than adjacent upper layer, positive values indicate  $T$  or  $\psi$  is higher at depth than adjacent upper layer

<sup>b</sup> Warren et al. (2005)

<sup>c</sup> Based on  $\rho_b$  and soil texture using ROSETTA 1.2 software (US Salinity Laboratory ARS-USDA, Riverside, CA, USA)

<sup>d</sup> Derived from Warren et al. (2005) using updated estimates of  $\theta_s$

<sup>e</sup> Equation 6.12a, Campbell (1985)

have previously established at this site (Warren et al. 2005). This improved model (Moldrup et al. 2000) was used to estimate  $D$  at each depth:

$$D = D_0(2\varepsilon_{100}^3 + 0.04\varepsilon_{100})\left(\frac{\varepsilon}{\varepsilon_{100}}\right)^{2+3/b} \quad (4)$$

where  $D_0$  is the diffusion coefficient of water vapor in air, taken as  $2.40 \times 10^{-5} \text{ m}^2 \text{ s}^{-1}$  at  $20^\circ\text{C}$  and 0.1 MPa adjusted to site  $T$  and altitude (915 m) using Campbell and Norman (1998),  $b$  represents the soil water retention parameter (Campbell 1974) calculated as the slope of the log–log soil water retention curve (Table 1; data derived from Warren et al. 2005),  $\varepsilon_{100}$  is the gas filled porosity at  $-100 \text{ cm H}_2\text{O}$  (extracted from the soil water retention curve) and  $\varepsilon$  is gas filled porosity as affected by soil volumetric water content ( $\theta$ ) and soil bulk density ( $\rho_b$ ; estimated from depth-based regression using data from Warren et al. 2005). Particle density of soil minerals ( $\rho_s$ ) is assumed to be  $2.65 \text{ mg m}^{-3}$  (Campbell 1985):

$$\varepsilon = 1 - \frac{\rho_b}{\rho_s} - \theta \quad (5)$$

An estimate of water vapor density can be generated by utilization of known relationships between  $\rho_v$ ,  $T$ , and water potential ( $\psi$ ) (Campbell and Norman 1998). These relationships can be expressed by:

$$\rho_v = \frac{h_r e_s(T) M_w}{RT_K} = \frac{\left(\exp\left(\frac{M_w \psi}{\rho_w RT_K}\right)\right) \left(a \exp\left(\frac{bT_C}{T_C + c}\right)\right) M_w}{RT_K} \quad (6)$$

where  $h_r$  is relative humidity,  $e_s(T)$  is the saturation vapor pressure at ambient  $T$  estimated using Tetens formula with constants  $a = 0.61121 \text{ kPa}$ ,  $b = 17.368$  and  $c = 238.88$  for  $T > 0$  (Buck 1981),  $M_w$  is the molecular weight of water ( $0.01802 \text{ kg mol}^{-1}$ ),  $\rho_w$  is the density of water ( $\text{kg m}^{-3}$ ),  $R$  is the gas constant ( $8.314 \text{ J mol}^{-1} \text{ K}^{-1}$ ),  $\psi$  (Pa) is the soil water matric potential, and  $T_C$  and  $T_K$  are both soil  $T$  with the subscripts C and K signifying units in Celsius or Kelvin, respectively.

The second term in Eq. 3 accounts for non-isothermal vapor flux which in the upper soil profile may be significant due to large diel  $T$  variations.  $\Delta T$  is the  $T$  difference across distance  $\Delta x$ ,  $h_r$  is relative humidity, and  $s$  is the slope of the saturation vapor concentration function ( $s = \Delta P$ ) (Campbell 1985; Bittelli et al. 2008), where  $P$  is barometric pressure (Pa) and  $\Delta$  is the slope of the saturation vapor pressure curve (Pa) at  $T$  using Tetens constants ( $b$  and  $c$ ) described earlier:

$$\Delta = \frac{bce_s(T)}{(c + T_C)^2} \quad (7)$$

Calculated vapor flux can be less than measured vapor flux by an order of magnitude, possibly due to  $\Delta T$  across

individual soil pores that leads to enhanced water transport through liquid-filled pores by condensation at one side of the pore and evaporation at the other side of the pore (Rose 1968a, b). A vapor enhancement factor ( $\eta$ ) can be estimated by knowledge of  $\theta$  and soil texture (Campbell 1985), and was applied as a correction factor to thermal diffusivity in Eq. 3, where  $\eta = A + B\theta - (A - D)\exp[-(C\theta)^E]$ , with constants  $A = 9.5$ ,  $B = 6$ ,  $D = 1$ ,  $E = 4$  and with  $C$  based on the clay fraction of soil ( $m_c$ ) (Cass et al. 1984; Campbell 1985),  $C = 1 + 2.6(m_c)^{-0.5}$ .

Liquid flux density ( $J_l$ ) within the upper soil layers was estimated during periods of apparent HR to investigate how much of the diurnal increase in soil moisture may be attributable to liquid water flux. Unsaturated flow ( $J_l$ ) is affected by soil texture, moisture content and driven by soil  $\psi$  gradients. Based on Darcy’s law, simple two-dimensional isothermal liquid flux density between two points in the soil is described by:

$$J_l = -k(\theta) \frac{\Delta\psi}{\Delta x} \quad (8)$$

where  $\Delta\psi$  is the water potential difference ( $\text{J kg}^{-1}$ ) over distance  $\Delta x$  (m) between measurement points, and  $k$  is unsaturated hydraulic conductivity ( $\text{kg s m}^{-3}$ ) at some  $\theta$  (Campbell 1985; Campbell and Norman 1998). The Brooks and Corey (1964) function for  $k(\theta)$  was extracted from prior analysis at the site (Warren et al. 2005):

$$k = k_s \left(\frac{\theta - \theta_r}{\theta_s - \theta_r}\right)^{\lambda+3} \quad (9)$$

$k$  is based on residual ( $\theta_r$ ) and saturated ( $\theta_s$ ) soil water content ( $\text{cm}^3 \text{ cm}^{-3}$ ),  $\lambda$  (related to texture) and saturated hydraulic conductivity ( $k_s$ ;  $\text{kg s m}^{-3}$ ; Campbell 1985):

$$k_s = 0.004 \left(\frac{1.3}{\rho_b}\right)^{1.3b} \exp^{(-6.9m_c - 3.7m_s)} \quad (10)$$

$k_s$  depends on bulk density ( $\rho_b$ ;  $\text{g cm}^{-3}$ ), and  $m_c$  and  $m_s$  the clay and silt soil fractions, respectively. While non-isothermal liquid flux is also part of the complete theory of Philip and de Vries (1957), its contribution under dry conditions is minimal compared with that driven by  $\psi$  gradients (Rose 1968b), and was not included in the model.

Net water storage ( $S$ ;  $\text{cm}^3 \text{ cm}^{-3}$ ),  $S = (J_v + J_l)_{\text{in}} - (J_v + J_l)_{\text{out}}$ , was calculated for each 10 cm depth layer every  $\frac{1}{2} \text{ h}$  during the 2002 growing season. Daily increases in modeled  $\theta$  within each soil layer were assessed by summation of  $S$  for the  $\frac{1}{2} \text{ h}$  periods when measured  $\theta$  was increasing. Total net increase in  $\theta$  within the upper 15–65 cm soil layer was assessed by summation of  $S$  in each soil layer. There were several occasions where calculations could not be performed due to sensor malfunctions or power loss.

In order to account for uncertainty in estimates of  $J_l$ ,  $J_v$  and  $J_{\text{total}}$ , we conducted a sensitivity analysis of the three key parameters used in this modeling exercise. Mean values  $\pm$  variability (as actual minimum and maximum values), or modeled confidence intervals (at 10 cm) in  $\psi$ ,  $\theta$  and  $T$  were individually propagated through the model equations to discern the potential influence of each parameter on water flux. The sensitivity analysis was conducted for net flux within the 20 cm layer (which displayed the largest range in parameter values) early (DOY 195) and late (DOY 290) in the season to establish parameter variation on modeled flux.

#### Estimates of hydraulic redistribution

Apparent HR of soil water has been previously calculated for this site based on measured daily recovery in  $\theta$  ( $\Delta\theta$ ) within each soil layer (Warren et al. 2005, 2007). To separate the potential contributions of vapor ( $J_v$ ) or liquid ( $J_l$ ) soil water flux to actual root HR, calculated  $J_v$  and  $J_l$  within each layer were subtracted from patterns of measured  $\theta$  during the assumed period of HR (increasing  $\theta$ ); the remaining diurnal variation in  $\theta$  was assumed to be HR. Net values of HR,  $J_v$  and  $J_l$  were calculated for each 10-cm depth interval from 15–65 cm at 30-min intervals. Values from each layer were summed to yield total flux within the 15–65 cm soil layer. Since the timing of HR,  $J_v$  and  $J_l$  varied for each soil layer, a portion of the reported total net daily values represent inter-layer transfers of water (e.g.,  $\theta$  declining in the 25–35 cm layer while simultaneously  $\theta$  increasing in the 15–25 cm layer). Data manipulation, modeling and regressions were performed with SAS software (version 9.1; SAS Institute, Cary, NC, USA) or SigmaPlot (Systat Software, Chicago, IL, USA).

## Results

In 2002, measured daily recovery in soil water content ( $\Delta\theta$ ) exceeded 0.05 mm day<sup>-1</sup> at specific 10-cm depth intervals and reached 0.18 mm day<sup>-1</sup> for the entire 50 cm soil layer (15–65 cm) by early August. Modeled liquid and vapor flux accounted for up to 20% of this  $\Delta\theta$  from August to November. The remaining 80+% of the  $\Delta\theta$  was considered to be HR of soil water by roots. Modeled soil liquid–water transport overshadowed HR earlier in the season under moister conditions, but was negligible later in the season.

Sensor precision was sufficient to quantify the small fluxes in  $\psi$  and  $\theta$  occurring over each ½ h interval. Laboratory-calibrated psychrometer sensors can accurately measure  $\psi$  to  $\pm 0.1$  MPa between 0 and  $-3.5$  MPa (Brown and Bartos 1982). The effective precision of field-deployed sensors during 2002 was found to be  $\pm 0.01$  MPa

(e.g.,  $\psi = -1.04 \pm 0.01$  MPa), which enabled accurate quantification of diurnal fluctuations in  $\psi$ , where daily recovery in  $\theta$  has been considered indicative of HR (Fig. 1). Nonlinear regression estimates of  $\psi$  at 2 and 10 cm were significant ( $R^2 = 0.71\text{--}0.81$ ,  $P < 0.001$  for regression parameter estimates of  $y_0$  and  $a$ , and  $P = 0.015\text{--}0.16$  for  $b$ ). Significance increased as soil dried and values with respect to  $\psi$  at 20 cm were conserved over the course of the summer; i.e., mean ( $\psi_{10}:\psi_{20}$ ) = 1.29 (range 1.17–1.55) and mean ( $\psi_2:\psi_{20}$ ) = 1.56 (range 1.34–2.12). FDC sensor resolution increases as soil dries (Dean et al. 1987), which coincides with development of the  $\psi$  gradients necessary for HR. The effective precision of the FDC sensors was  $\pm 0.032\text{--}0.012\%$  for  $\theta$  ranging from 0.05 to 0.55 cm<sup>3</sup> cm<sup>-3</sup>, respectively (e.g.,  $\theta = 0.10125 \pm 0.00002$  cm<sup>3</sup> cm<sup>-3</sup>), which enabled very accurate quantification of diurnal  $\theta$  fluctuations assumed to represent HR (Fig. 1) (Brooks et al. 2002; Warren et al. 2007). Linear regression estimates of  $\theta$  were significant and uniform throughout the season (mean  $R^2 = 0.96$ ; slope = 0.22,  $P < 0.05$ ).  $\theta$  at 10 cm with respect to  $\theta$  at 20 cm ( $\theta_{10}:\theta_{20}$ ) was  $0.50 \pm 0.02$  (range 0.37–0.60); ( $\theta_2:\theta_{20}$ ) was  $0.22 \pm 0.03$  (range 0.09–0.29).

The largest potential source of error in the FDC sensors was due to soil  $T$  fluctuations. The magnitude of  $T$  corrections to  $\theta$  declined (from 0.089 to 0.021% °C<sup>-1</sup>) as soil  $\theta$  declined (from 0.167 to 0.060 cm<sup>3</sup> cm<sup>-3</sup>) based on 60 MHz FDC sensors calibrated in sand (Kuráň 1982). Estimates were similar to other correction factors based on 150 MHz FDC sensors calibrated in air-dry soil (0.027% °C<sup>-1</sup>; Dean et al. 1987) or in water (0.19% °C<sup>-1</sup> at 0.167 cm<sup>3</sup> cm<sup>-3</sup>; Paltineanu and Starr 1997). The two latter studies did not  $T$ -calibrate sensors across a range of soil  $\theta$ , which limits extension to other values of  $\theta$ . Nonetheless,  $T$ -correction values for Dean et al. (1987) using dry soil ( $<0.04$  cm<sup>3</sup> cm<sup>-3</sup>) were consistent with our estimates for similarly dry soil (0.06 cm<sup>3</sup> cm<sup>-3</sup>) based on Kuráň (1982). Our  $T$  calibration of 150 MHz FDC sensors using moistened sand (0.0303 cm<sup>3</sup> cm<sup>-3</sup>; 0.021–0.075% °C<sup>-1</sup>; ESM1, Online Resource) also agreed with the calibrations of Kuráň (1982).

Absolute values of  $\theta$  were not strongly affected by the  $T$  corrections, in agreement with a previous report of the  $T$ -insensitivity of FDC sensors (Paltineanu and Starr 1997); however, small relative changes in  $\theta$  over time can be affected by large  $T$  shifts. For example, nocturnal increases in  $\theta$  can occur over an 8-h period during which time soil  $T$  may decline by 3°C or more. Assuming actual  $\theta$  remains constant (e.g., 0.10000 cm<sup>3</sup> cm<sup>-3</sup>), a 3°C decline results in measured output of 0.10014 cm<sup>3</sup> cm<sup>-3</sup>, which would appear as a 0.00014 cm<sup>3</sup> cm<sup>-3</sup> (0.014 mm per 10 cm depth) increase in  $\theta$  ( $\Delta\theta$ ). At our site, the amount of soil  $T$  decline during the night, if not accounted for, could result

in a potential overestimation of  $\Delta\theta$ . Minimum soil  $T$  was usually reached prior to maximum  $\theta$  at a particular depth, which reduced some of the  $T$ -dependent error in  $\Delta\theta$ .  $T$ -correction in sensor output led to a 30% increase in calculated  $\Delta\theta$  in late spring (DOY 145) as compared to uncorrected values. The magnitude of  $\Delta\theta$  increased during the summer and peaked at  $0.18 \text{ mm day}^{-1}$  by DOY 210, by which point the impact of  $T$ -corrections were relatively minor ( $\sim 5\%$ ) (Fig. 2).

The upper soil layers experienced large diurnal and seasonal shifts in  $T$  that regulated water vapor flux ( $J_v$ ) dynamics within the soil profile. Diurnally, the upper soil layer experienced the largest  $T$  gradients: soil  $T$  at 10 cm depth was up to  $17.3^\circ\text{C}$  cooler than  $T$  at 2 cm (daytime) and up to  $8.6^\circ\text{C}$  warmer than  $T$  at 2 cm (nighttime) (Table 1). Maximum  $T$  at 2 cm peaked above  $37^\circ\text{C}$  in late July (min  $10^\circ\text{C}$ ), then declined to  $10^\circ\text{C}$  by early October (min  $-1^\circ\text{C}$ ). Seasonally, soil  $T$  at 20 cm depth ranged from 5 to  $20^\circ\text{C}$  between June and November.  $J_v$  was strongly dependent on soil  $T$  differences between layers that controlled magnitude and direction of flow (upward or downward; Fig. 3). Soil  $T$  differences and  $J_v$  between layers dampened with depth. Maximum daily  $T$  fluctuations measured during the period of HR at 20 cm depth were up to  $\sim 7^\circ\text{C}$ , whereas at 60 cm depth were less than  $2^\circ\text{C}$  (Table 1; Fig. 3).

The direction of  $J_v$  shifted daily and at different times in different soil layers which resulted in concurrent upward fluxes in some layers and downward fluxes in other layers. In fact, high daytime surface  $T$  resulted in a relatively large influx of water into the 10 cm soil layer as soil moisture was driven downward from the upper few cm during the day. The time course of  $J_v$  at 10 cm modeled using data collected in 2002 when  $\theta$  was measured only from 20 to 60 cm (Fig. 4 upper) was consistent with that of the

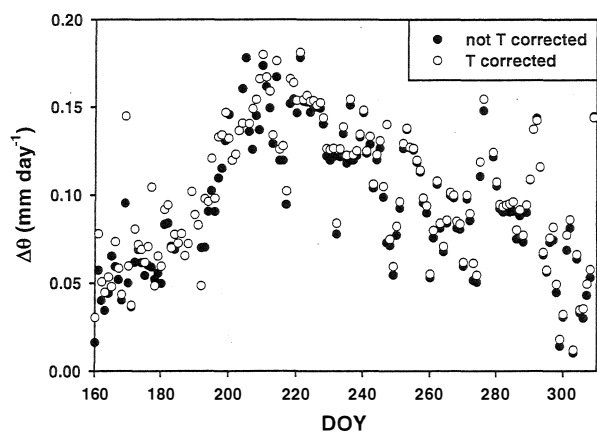


**Fig. 2** Total daily recovery in upper soil water content (15–65 cm) based on frequency domain capacitance sensors with and without temperature corrections applied to sensor output

$T$ -corrected, measured  $\Delta\theta$  at 10 cm under similar conditions in 2000 (Fig. 4, lower). Time courses of measured  $\Delta\theta$  and modeled  $J_v$  at 10 cm were offset from those at 30 cm,

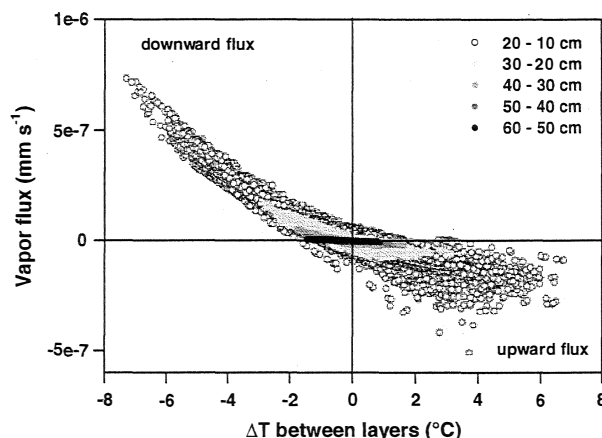


**Fig. 3** Net vapor flux between adjacent soil layers at 30-min intervals relative to temperature gradients in the system

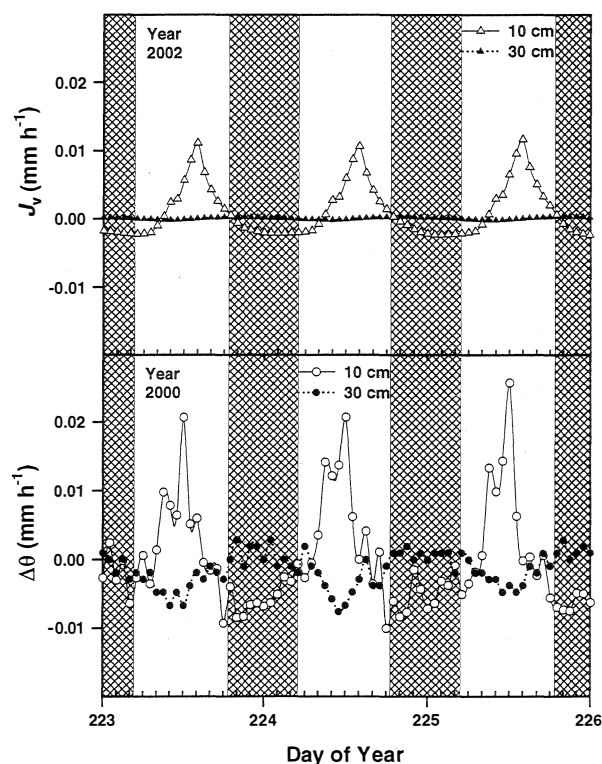


**Fig. 4** Upper Modeled vapor flux ( $J_v$ ) for 10 and 30 cm depths in year 2002 based on measurement of temperature throughout the profile, and measurement of soil water content and water potential from 20 to 60 cm depth ( $n = 4-6$ ). Lower Measured,  $T$ -corrected soil water flux observed at 10 and 30 cm depth in an old-growth ponderosa pine site in year 2000. The sensor at 10 cm depicts increasing water content during the day, offset from typical patterns exhibited in deeper soil layers that decline during the day as roots extract water to supply transpirational demand

and vapor fluxes at 10 cm were greater than those at 30 cm (Fig. 4).

The magnitude of  $J_v$  was also regulated by  $D$  and by the vapor enhancement factor ( $\eta$ ). The  $\eta$  that was applied to the thermal diffusivity term in Eq. 3 ranged from  $-1.4$  to  $11$ , with the highest values early in the season at the deeper depths. At the 10 cm depth, lower clay content and drier conditions led to  $\eta$  ranging from 6 (early June) to 2 (mid-July) to 1.4 (late August).  $\eta$  at 20 cm declined from 10 to 2.4 by the end of the season,  $\eta$  at 30 cm declined to 5.9, while  $\eta$  for depths  $>40$  cm remained close to 10. Since the timing, magnitude and direction of  $J_v$  varied substantially between layers, the net impact of  $\eta$  for the entire 15–65 cm profile ranged from a 60% decrease in the non-isothermal vapor flux (early season) to a 20% increase (late season). The contribution of non-isothermal vapor flux to total  $J_v$  (isothermal + non-isothermal) was seasonally dynamic, and ranged from 5 to 30% of total  $J_v$ .

Large diurnal and seasonal shifts in  $\theta$  and  $\psi$  in the upper soil layers also regulated liquid water ( $J_l$ ) flux dynamics within the soil profile. Soil  $\theta$  at 10 cm was 30–50% lower than soil  $\theta$  at 20 cm, and soil  $\psi$  at 10 cm was 20–40% lower than soil  $\psi$  at 20 cm. Soil  $\psi$  at 2 cm depth was up to 3.3 MPa more negative (drier) than at 10 cm depth (Table 1). As soil dried, seasonal development of large  $\psi$  gradients within the soil profile created a driving force for

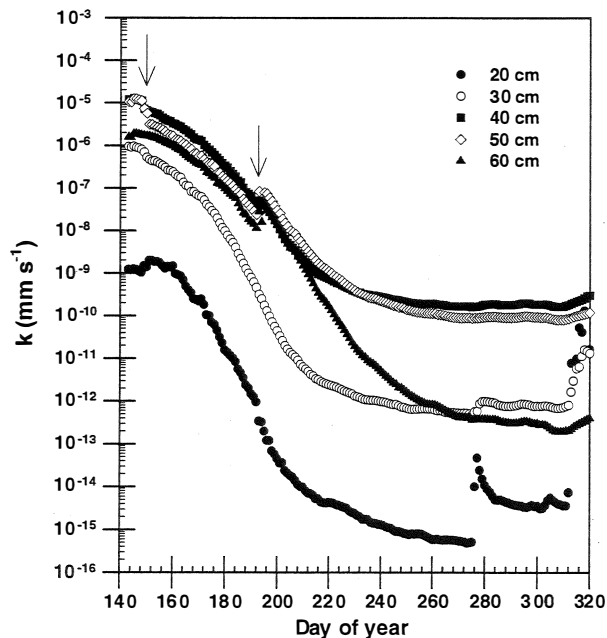


**Fig. 5** Unsaturated soil hydraulic conductivity ( $k$ ) at multiple depths across a seasonal dry period in 2002. Arrows indicate the result of moving one  $\theta$  probe between two locations several meters apart. Standard error of the four probes varied by date and depth;  $SE$  was 1–11% of  $k$

unsaturated water transport between soil layers, but also led to exponential declines in hydraulic conductivity ( $k$ ) (Fig. 5). These contrasting controlling factors often counteracted one another. For example, the  $\psi$ -difference between the 50–60 cm soil layers increased four-fold between DOY 210 and DOY 220, but  $k$  concurrently decreased by a factor of four such that net  $J_l$  between these deep layers did not change.

Early in the season, modeled  $J_v$  and  $J_l$  exceeded measured  $\Delta\theta$  in the upper soil.  $J_v$  could account for up to 15% of  $\Delta\theta$ , while potential  $J_l$  was up to four-fold greater than measured  $\Delta\theta$  and varied between influx into the profile and efflux from the profile (Figs. 6 and 7). The magnitude of  $J_l$  in comparison with  $\Delta\theta$  suggests that root HR, as water release via the root system, and root water extraction were significant and contributed to net variability in upper soil  $\theta$ . By early August,  $\Delta\theta$  was reaching its seasonal peak (Fig. 7), while modeled  $J_l$  declined to less than 10% of measured  $\Delta\theta$  (Fig. 6, inset), remaining a small component of the upper soil water budget through the end of the dry season.

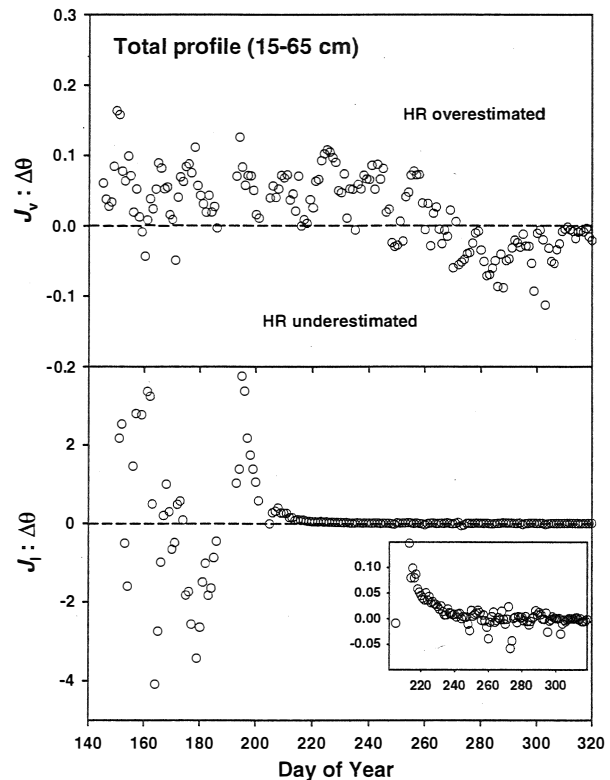


**Fig. 6** Net relative contribution of vapor ( $J_v$ ) or liquid ( $J_l$ ) water flux to measured daily recovery in soil water content ( $\Delta\theta$ ) throughout the upper soil profile. Estimates of root hydraulic redistribution (HR) based solely on  $\Delta\theta$  are confounded by these mechanisms when  $J \neq 0$ , resulting in overestimation or underestimation of HR. Negative values represent water transport out of the profile, positive values represent water transport into the profile

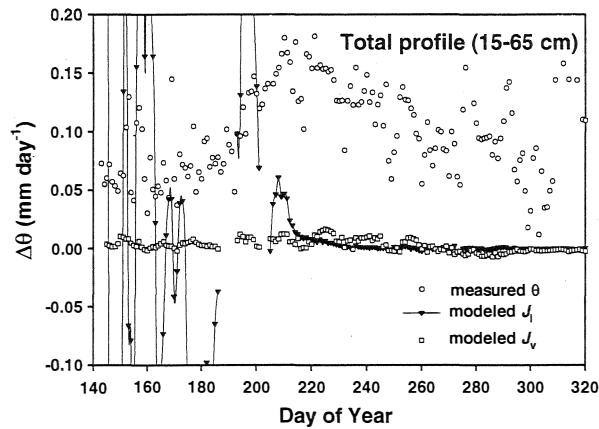


**Fig. 7** Seasonal patterns of measured and modeled daily recovery in soil water content ( $\Delta\theta$ ) in the 15–65 cm soil profile. Measured values ( $\theta$ ) were dominated by liquid flux ( $J_1$ ) early in the season; vapor flux ( $J_v$ ) was more important to  $\theta$  later in the season. The difference between  $\theta$  and  $J_1 + J_v$  is presumed to be hydraulic redistribution by roots

It is likely that spatial heterogeneity in actual values and measurement of soil  $T$ ,  $\psi$  and  $\theta$  (and thus  $k$ ) precluded accurate measurement of interlayer fluxes early in the season, which led to overestimates of net  $J_1$  through the profile. Despite lower  $\psi$  in the upper soil layers, net  $J_1$  within a layer was driven by higher  $k$  in the adjacent, deeper soil layer; i.e.,  $J_1$  at 20 cm was 2–3 orders of magnitude lower than  $J_1$  at 30 cm. Errors in  $\psi$  and  $k$  were less relevant to total water flux late in the season as  $J_v$  increased in dominance. The maximum impact of variability in  $\psi$  at 10 cm on  $J_1$  was <2%, and on  $J_v$  was 1.2–6.4% as the season progressed. The impact in  $\psi$  at 20 cm on  $J_1$  ranged from 182 to 484% (DOY 195–290), and on  $J_v$  was 0.5–2.2%; this represented a potential impact of 13% of  $J_{total}$  (total flux) DOY 195, declining to <3.2% by DOY 290. The maximum impact of variability in  $\theta$  at 10 cm on  $J_1$  and on  $J_v$  was <3% throughout the season. The impact in  $\theta$  at 20 cm on  $J_1$  ranged from 335 to 289% (DOY 195–290), and on  $J_v$  was 3.3–3.0%; this represented a potential impact of 57% of  $J_{total}$  (total flux) DOY 195, declining to <3.2% by DOY 290. The greatest potential source of variation in model output was upper soil  $T$ . The maximum potential impact of measurement error (or variability) in  $T$  at 10 cm on  $J_v$  (and  $J_{total}$ ) was ~25% on DOY 290, shifting from +25% in the morning to -24% late in the day. Error in  $T$  at deeper depths was <3.2%.

Seasonal patterns and magnitude of  $\Delta\theta$  varied by depth (Fig. 8).  $\Delta\theta$  was relatively small during late May throughout the profile, and primarily driven by  $J_1$ . The contribution of  $J_1$  to  $\Delta\theta$  decreased as soils dried and uncovered the underlying patterns of  $J_v$ , whose relative contribution to  $\Delta\theta$  greatly exceeded that of  $J_1$  during the period of HR. Based on the modeled fluxes and subtracting

them from  $\Delta\theta$  to estimate HR, HR was equal to, greater than, or less than measured  $\Delta\theta$  in the soil, depending on depth and time into the drying cycle (Fig. 8). For example, HR increased from 0 to 90% of  $\Delta\theta$  at 40 cm depth from DOY 200 to DOY 250, HR was 5–50% greater than  $\Delta\theta$  at 50 cm depth throughout the season, and HR was equal to  $\Delta\theta$  at 60 cm depth after DOY 220 (Fig. 8).

Total calculated HR throughout the upper 15–65 cm layer was difficult to assess prior to DOY 206 when HR accounted for ~65% of  $\Delta\theta$  (Fig. 9). Earlier in the season, values for HR: $\Delta\theta$  ranged from -3 to 5, suggesting that large variability in parameter estimates for each layer led to accumulated errors at the profile level, which were exacerbated by relatively small values of  $\Delta\theta$ . By August (DOY 213), at the time of maximum measured  $\Delta\theta$ , HR could account for at least 80%, and up to 111% of the daily recovery in  $\theta$  throughout the upper 15–65 cm soil profile (Fig. 9). Large deviations between  $\Delta\theta$  and HR occurred

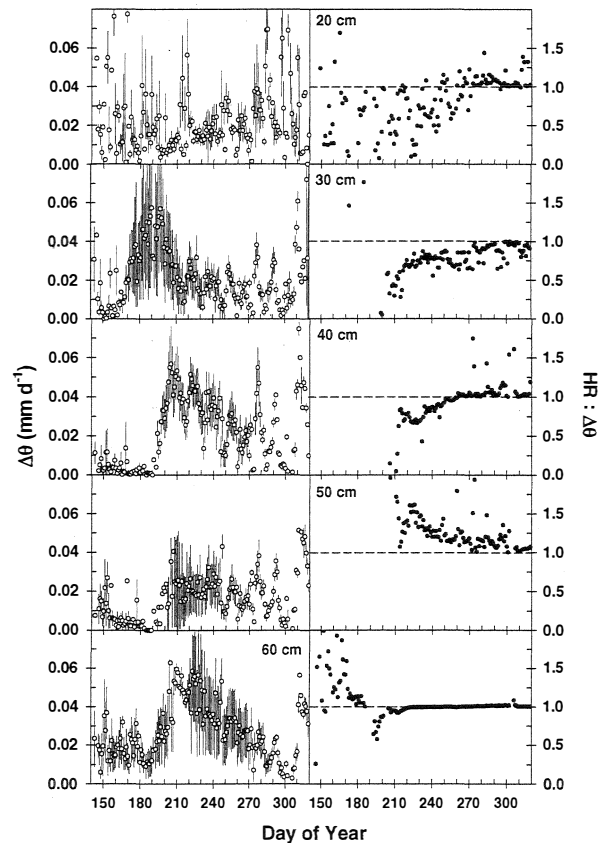


**Fig. 8** *Left* Seasonal patterns of measured daily recovery in soil water content ( $\Delta\theta$ ) by depth. Each value represents four sensors centered at a particular depth,  $\pm$ SE. *Right* Total calculated hydraulic redistribution (HR) relative to measured flux ( $\Delta\theta$ ); where values >1 suggest HR is greater than  $\Delta\theta$ , while values equal to 1 suggest HR is 100% of  $\Delta\theta$ . Missing values early in the summer for the 30–50 cm depths were either <0 suggesting negative HR (i.e., root water uptake) or >2 due to a small value of  $\Delta\theta$  in the denominator

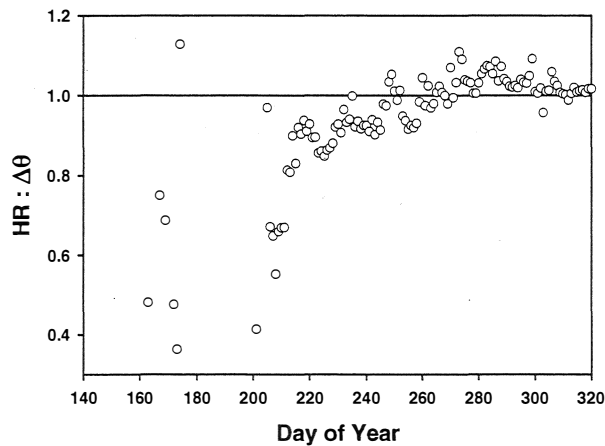


**Fig. 9** Seasonal patterns in modeled HR in the upper 15–65 cm soil layer with respect to daily recovery in soil water content ( $\Delta\theta$ ). Values of  $HR/\Delta\theta < 1$  signify conditions where measurements would overestimate HR if vapor flux were not taken into account; the converse for values of  $HR/\Delta\theta > 1$

primarily during moist conditions with relatively frequent precipitation inputs, early in the season or after the droughty period ended (DOY 273).

## Discussion

Separately accounting for the various mechanisms contributing to changes in soil moisture, including HR, liquid and vapor fluxes of soil water, is critical for understanding and modeling water dynamics and understanding the implication of these dynamics across multiple scales—ranging from microscopic soil rhizosphere processes to soil–plant water exchange dynamics, and whole ecosystem and landscape level water transport. Quantifying fluxes within the soil–plant–atmosphere continuum continues to be a challenge, particularly for small-scale fluxes within and between specific components; e.g., two soil layers, soil–root, canopy–atmosphere. Large spatial heterogeneity of soil and plant physical characteristics, interactions between components, and temporal influence of environmental conditions underscores the complexity of response across a landscape. Modeled soil water transport within the soil profile is dependent on variation in measured sensor responses, parameter estimates, and simultaneous calculation of liquid and vapor flux upward and downward within the soil profile. Resultant net transport within a specific soil layer thus reflects large and cumulative error from many sources that is exacerbated during periods of precipitation inputs or rapid changes in weather, and confounded by root water extraction or release. As soils dried in our old-growth pine ecosystem, soil water transport between layers and root water release by HR could be separately quantified by

the model, substantiating prior assumption and evidence of HR at the site, and providing a method to further refine estimates of the magnitude of HR across ecosystems.

For this exercise, vapor transport was considered to be driven entirely by molecular diffusive processes. Advection was not considered, but may also be a component of vapor transport in the uppermost layers where rapid thermal expansion or contraction of water vapor due to direct surface–atmosphere heat exchange (including solar heating of the soil surface) can contribute to net transport, as well as pressure pulses associated with storm fronts. Advection has been proposed as a missing component of the Philip and de Vries (1957) vapor transport model, perhaps replacing the vapor enhancement correction factor (Cahill and Parlange 1998; Parlange et al. 1998), although its applicability has not been resolved or verified (Or and Wraith 2000; Bittelli et al. 2008), and its importance may be minor (Rose 1968b). Our analysis modeled simple diffusive vapor flow and unsaturated liquid water flow  $J_v$  and  $J_l$ , based on  $T$ ,  $\psi$  and  $\theta$  data, between soil layers to identify the relative contribution of root HR to nocturnal water release in the upper soil.

In the spring and early summer, the magnitude and variability of modeled unsaturated soil water flux between soil layers limited the separation of root and soil contributions to  $\Delta\theta$ .  $J_l$  was strongly dependent on saturated and unsaturated hydraulic conductivity and declined rapidly as soils dried such that its confounding impact on estimates of HR was fully dissipated by midsummer.

Diurnal patterns of surface warming and cooling and the resultant thermal wave that propagates into the soil profile control soil water content in the upper 5–15 cm by regulation of soil water vapor flux. This water flux is independent of HR which has been previously determined to decrease seasonally in the upper 20 cm due to xylem embolism in fine roots under drying conditions (Domec et al. 2004; Warren et al. 2007). The relatively slow vertical propagation of the thermal wave results in some soil layers that were cooling while other soil layers were warming. Thus, depending on the relative  $T$  differences between layers, vapor flow was moving simultaneously upward into one soil layer and downward into adjacent soil layers—a process that is independent of root-mediated flux into the soil as HR or out of the soil as transpiration.

Temperature can impact soil permittivity and FDC or time-domain reflectometry (TDR) sensor responses that can result in unrealistic patterns of  $\theta$  if not corrected (Wraith and Or 1999; Verhoef et al. 2006). The response of 150 MHz FDC sensors closely tracked changes in soil  $T$  in sealed, air-dry loam soil columns ( $1.39 \text{ g cm}^{-3}$ ; 13–27% clay) (Baumhardt et al. 2000). The diel  $T$  fluctuations ranged from 20 to 25°C and resulted in <0.1% change in apparent  $\theta$ , which reflects the impact of  $T$  on FDC sensor

response to changes in soil permittivity, as well as actual changes in  $\theta$  as small amounts of water vapor moved within the sealed column. Apparent  $\theta$  based on TDR depends on altered signal propagation due to  $T$ -induced shifts in bound: unbound soil water, especially for soils high in surface area (e.g., clay; Wraith and Or 1999). In their study with loamy sand soil (3% clay), there was no definitive change in the measured dielectric constant with  $T$ -shifts between 5 and 20°C (the diurnal  $T$  range of our soils >10 cm deep) for  $\theta = 0.05$  or  $0.20 \text{ cm}^3 \text{ cm}^{-3}$ . Our sandy loam soils were also low in clay (4–6% in the upper 60 cm; Warren et al. 2005), and lower in  $\rho_b$  than the Baumhardt et al. (2000) study, which may limit this type of unaccounted  $T$ -dependent error in our study.

Data collected previously from this pine site (Brooks et al. 2002), from a nearby *Juniperus occidentalis* site (J. Warren, unpublished), and from a young *Pseudotsuga menziesii* stand (Brooks et al. 2006) include evidence of increases in soil water content during the daytime in the upper 5–15 cm layer, a time when actively transpiring trees should be reducing soil water content. At the sandy *J. occidentalis* site, FDC sensors installed between 0 and 20 cm depth exhibited large daytime increases in  $\theta$  that peaked at 1600 hours then declined until ~0200 hours. At the pine site, soil  $\theta$  at 10 cm began to increase at 0800 hours, then peaked at 1500 hours; soil  $\theta$  at 20 cm began to increase at 1400 hours, then peaked at 2300 hours. Deeper depths (30–100 cm) displayed typical patterns of HR, in which  $\theta$  increased at 1900–2200 hours, then declined at 0700–0800 hours. The ‘apparent’ daytime HR in the upper 0–20 cm layers was thus out of phase from normal patterns of nocturnal HR concurrently described in deeper layers. In addition, the magnitude of the increase in  $\theta$  was often quite large, much greater than nocturnal HR exhibited in deeper soil layers. This daytime increase in soil  $\theta$  (or  $\psi$ ) has also been reported at deeper depths, including in *Quercus douglasii* (Millikin-Ishikawa and Bledsoe 2000) and mixed *P. ponderosa*–*Quercus* sp. (Espeleta et al. 2004), and described as “offset fluctuations” (Millikin-Ishikawa and Bledsoe 2000). In these studies, including our own, the daytime increases in  $\theta$  were often correlated to soil  $T$ , and much of the apparent change in  $\theta$  may be directly attributable to  $T$  sensitivity of the measurement sensors (cf. Verhoef et al. 2006). Nonetheless, a daytime increase in upper soil  $\theta$  can also be attributed to soil thermal gradients that drive vapor flux into upper soil, which has been previously demonstrated gravimetrically (e.g., Jackson 1973) or calculated (e.g., Bruce et al. 1977). Thus, direct  $T$  impacts on sensor response do not entirely account for the increases in daytime  $\theta$  apparent in these studies.

The daytime increases in  $\theta$  in the shallowest soil layers (<15 cm depth) may be explained by the balance of heat

flux within the soil profile under dry conditions and a deep water table (Philip 1957). Solar radiation can heat these upper soil layers during the day that creates conditions for potential evaporation and upward loss of water, yet deeper (e.g., >15 cm) soil  $\theta$  and  $T$  may be low enough that net vapor water flux is downward (e.g., Jackson 1973). Subsequently, at night, atmospheric  $T$  may decline (by up to 25°C in late summer at our pine site), which creates a net driving force for evaporative water flux out of upper soil.  $T$  differences between adjacent layers deeper in the profile are small in comparison, and diurnal  $\theta$  follows typical patterns: extraction by roots during the day, recharge as HR and soil water flux at night. The diurnal  $T$  gradients within the upper soil were as high as 17°C (i.e., between 2 and 10 cm depth; Table 1), and temporal dynamics of these gradients allowed for net vapor flux into the upper soil during the day. Thus, in this study, and likely in other studies, vapor flux can account for a substantial portion of the ‘offset patterns’ that we and others have previously considered solely measurement errors.

## Conclusions

Diurnal  $\theta$  patterns measured in the upper soil have been attributed to various mechanisms, including direct  $T$ -dependence of permittivity or sensor response, soil  $J_1$ , soil  $J_v$ , root HR or root water extraction. Investigations of HR must include robust consideration of each of these components, their relative magnitudes and temporal significance. Our results agree with other methods that indicate that roots can contribute significantly to the diurnal patterns assumed to be HR and can be the dominant process behind  $\Delta\theta$  when soils are sufficiently dry. Seasonally, HR is an important component of the upper soil water budget that replaces much of the daytime depletion during droughty periods and enables prolonged root viability in the nutrient-rich upper soil. While the absolute magnitude of HR is not easily quantified, total diurnal fluctuations in upper soil water content can be quantified and modeled, and remain highly applicable for establishing the magnitude and temporal dynamics of total ecosystem water flux.

**Acknowledgments** We gratefully thank James Irvine and Bev Law for providing site data, including temperature profiles, and Rob Coulombe, J.C. Domec and David Woodruff for fieldwork. We appreciate comments from Gerald Flerchinger on an earlier version of this manuscript. This research was supported by the U.S. Department of Energy, Office of Science, Biological and Environmental Research Program, by the USDA Forest Service Ecosystem Processes Program and by the US Environmental Protection Agency. Oak Ridge National Laboratory is managed by UT-Battelle, LLC, for the U.S. Department of Energy under contract DE-AC05-00OR22725. This manuscript has been subjected to the Environmental Protection Agency’s peer and administrative review, and it has been approved for publication as an EPA document. Mention of trade names or commercial products does not constitute endorsement or recommendation for use.

## References

- Agam (Ninari) N, Berliner PR (2004) Diurnal water content changes in the bare soil of a coastal desert. *J Hydrometeorol* 5:922–933
- Baumhardt RL, Lascano RJ, Evett SR (2000) Soil material, temperature, and salinity effects on calibration of multisensor capacitance probes. *Soil Sci Soc Am J* 64:1940–1946
- Bittelli M, Ventura F, Campbell GS, Snyder RL, Gallegati F, Pisa PR (2008) Coupling of heat, water vapor, and liquid water fluxes to compute evaporation in bare soils. *J Hydrol* 362:191–205
- Brooks RH, Corey AT (1964) Hydraulic properties of porous media Hydrology Paper no 3. Civil Engineering Department, Colorado State University, Fort Collins
- Brooks JR, Meinzer FC, Coulombe R, Gregg J (2002) Hydraulic redistribution of soil water during summer drought in two contrasting Pacific Northwest coniferous forests. *Tree Physiol* 22:1107–1117
- Brooks JR, Meinzer FC, Warren JM, Domec JC, Coulombe R (2006) Hydraulic redistribution in a Douglas-fir forest: lessons from system manipulations. *Plant Cell Environ* 29:138–150
- Brown RW, Bartos DL (1982) A calibration model for screen-caged Peltier thermocouple psychrometers. USDA For Serv Res Pap INT-293 Ogden, UT, Intermt For and Range Exp Stn
- Bruce RR, Thomas AW, Harper LA, Leonard RA (1977) Diurnal soil water regime in the tilled plow layer of a warm humid climate. *Soil Sci Soc Am J* 41:455–460
- Buck AL (1981) New equations for computing vapor pressure and enhancement factor. *J Appl Meteorol* 20:1527–1532
- Burgess SSO, Pate JS, Adams MA, Dawson TE (2000) Seasonal water acquisition and redistribution in the Australian woody phreatophyte, *Banksia prinites*. *Ann Bot (London)* 85:215–224
- Cahill AT, Parlange MB (1998) On water vapor transport in field soils. *Water Resour Res* 34:731–739
- Caldwell MM, Richards JH (1989) Hydraulic lift: water efflux from upper roots improves effectiveness of water uptake by deep roots. *Oecologia* 79:1–5
- Caldwell MM, Dawson TE, Richards JH (1998) Hydraulic lift: consequences of water efflux from the roots of plants. *Oecologia* 113:151–161
- Campbell GS (1974) A simple method for determining unsaturated conductivity from moisture retention data. *Soil Sci* 117:311–314
- Campbell GS (1985) Soil physics with basic—transport models for soil—plant systems. *Developments in Soil Science*, 14. Elsevier, Amsterdam
- Campbell GS, Norman JM (1998) Introduction to environmental biophysics. Springer, New York, p 305
- Cass A, Campbell GS, Jones TL (1984) Enhancement of thermal water vapor diffusion in soil. *Soil Sci Soc Am J* 48:25–32
- Dawson TE (1993) Hydraulic lift and water use by plants: implications for water balance, performance and plant-plant interactions. *Oecologia* 95:565–574
- Dean TJ, Bell JP, Baty AJB (1987) Soil moisture measurement by an improved capacitance technique, part 1 sensor design and performance. *J Hydrol* 93:67–78
- Domec JC, Warren JM, Meinzer FC, Brooks JR, Coulombe R (2004) Native root xylem embolism and stomatal closure in stands of Douglas-fir and ponderosa pine: mitigation by hydraulic redistribution. *Oecologia* 141:7–16
- Espeleta JF, West JB, Donovan LA (2004) Species-specific patterns of hydraulic lift in co-occurring adult trees and grasses in a sandhill community. *Oecologia* 138:341–349
- Irvine J, Law BE, Anthoni PM, Meinzer FC (2002) Water limitations to carbon exchange in old-growth and young ponderosa pine stands. *Tree Physiol* 22:189–196
- Jackson RD (1973) Diurnal changes in soil water content during drying. In: Bruce RR, Flach KW, Taylor HM (eds) *Field soil water regime*. Soil Science Society of America, Fitchburg, pp 37–55
- Kuráz V (1982) Testing of a field dielectric soil moisture meter. *Geotech Test J* 4:111–116
- Law BE, Ryan MG, Anthoni PM (1999) Seasonal and annual respiration of a ponderosa pine ecosystem. *Global Change Biol* 5:169–182
- Law BE, Thornton PE, Irvine J, Anthoni PM, van Tuyl S (2001) Carbon storage and fluxes in ponderosa pine forests at different developmental stages. *Global Change Biol* 7:755–777
- Meinzer FC, Brooks JR, Bucci S, Goldstein G, Scholz FG, Warren JM (2004) Converging patterns of uptake and hydraulic redistribution of soil water in contrasting woody vegetation types. *Tree Physiol* 24:919–928
- Millikin-Ishikawa C, Bledsoe CS (2000) Seasonal and diurnal patterns of soil water potential in the rhizosphere and blue oaks: evidence for hydraulic lift. *Oecologia* 125:459–465
- Moldrup P, Olesen T, Schjonning P, Yamaguchi T, Rolston DE (2000) Predicting the gas diffusion coefficient in undisturbed soil from soil water characteristics. *Soil Sci Soc Am J* 64:94–100
- Morgan KT, Parsons LR, Wheaton TA, Pitts DJ, Obreza TA (1999) Field calibration of a capacitance water content probe in fine sand soils. *Soil Sci Soc Am J* 63:987–989
- Nakayama FS, Jackson RD, Kimball BA, Reginato RJ (1973) Diurnal soil-water evaporation: chloride movement and accumulation near the soil surface. *Soil Sci Soc Am Proc* 37:509–513
- Or D, Wraith JM (2000) Comment on “on water vapor transport in field soils” by Anthony T Cahill and Marc B Parlange. *Water Resour Res* 36:3103–3105
- Paltineanu IC, Starr JL (1997) Real-time soil water dynamics using multisensor capacitance probes: laboratory calibration. *Soil Sci Soc Am J* 61:1576–1585
- Parlange MB, Cahill AT, Nielsen DR, Hopmans JW, Wendroth O (1998) Review of heat and water movement in field soils. *Soil Till Res* 47:5–10
- Penman HL (1940) Gas and vapor movements in soil: the diffusion of vapors through porous solids. *J Agric Sci (Cambridge)* 30:437–462
- Philip JR (1957) Evaporation, and moisture and heat fields in the soil. *J Meteorol* 14:354–366
- Philip JR, de Vries DA (1957) Moisture movement in porous materials under temperature gradients. *Trans Am Geophys Union* 38:222–232
- Querejeta JI, Egerton-Warburton LM, Allen MF (2003) Direct nocturnal water transfer from oaks to their mycorrhizal symbionts during severe soil drying. *Oecologia* 134:55–64
- Richards JH, Caldwell MM (1987) Hydraulic lift: substantial nocturnal water transport between soil layers by *Artemisia tridentata* roots. *Oecologia* 73:486–489
- Rose CW (1968a) Water transport in soil with a daily temperature wave—1 Theory and experiment. *Aust J Soil Res* 6:31–44
- Rose CW (1968b) Water transport in soil with a daily temperature wave—2 Analysis. *Aust J Soil Res* 6:45–57
- Selker JS, Keller CK, McCord JT (1999) Vadose zone processes. Lewis, Boca Raton
- Verhoef A, Fernández-Gálvez J, Diaz-Espejo A, Main BE, El-Bishti M (2006) The diurnal course of soil moisture as measured by various dielectric sensors: effects of soil temperature and the implications for evaporation estimates. *J Hydrol* 321:147–162
- Warren JM, Meinzer FC, Brooks JR, Domec JC (2005) Vertical stratification of soil water storage and release dynamics in Pacific Northwest coniferous forests. *Agric For Meteorol* 130:39–58
- Warren JM, Meinzer FC, Brooks JR, Domec JC, Coulombe R (2007) Hydraulic redistribution of soil water in two old-growth

- coniferous forests: quantifying patterns and controls. *New Phytol* 173:753–765
- Warren JM, Brooks JR, Meinzer FC, Eberhart JL (2008) Hydraulic redistribution of water from *Pinus ponderosa* trees to seedlings: evidence for an ectomycorrhizal pathway. *New Phytol* 178: 382–394
- Wraith JM, Or D (1999) Temperature effects on soil bulk dielectric permittivity measured by time domain reflectometry: experimental evidence and hypothesis development. *Water Resour Res* 35:361–369